A Thiazolo[5,4-*d*]thiazole Functionalized Covalent Triazine Framework Showing Superior Photocatalytic Activity for Hydrogen Production and Dye Degradation

Hao Wang, [a] Lijiang Guan, [b] Jiawei Liu, [a] Tingting Lei, [a] Yuxin Xue, [a] Zhi Qu, [a] Shangbin Jin,*[b] Haixia Ma, [a] Zhaoqi Guo*[a]

[a.] School of Chemical Engineering / Xi'an Key Laboratory of Special Energy Materials, Northwest University, Xi'an 710069, Shaanxi, P. R. China. E-mail: zqguo@nwu.edu.cn

[b.] School of Chemical Engineering and Technology, Xi'an Jiaotong University, Xi'an 710049, Shaanxi, P. R. China. E-mail: shangbin@xjtu.edu.cn

Contents

1. Materials and Methods

1.1 Materials

All reagents and solvents were obtained from commercial suppliers and used as received: dichloromethane (DCM), N, N-dimethylformamide (DMF), tetrahydrofuran (THF), ethanol, methanol (MeOH), acetonitrile, dimethyl sulfoxide (DMSO) and o-dichlorobenzene (o-DCB), 1,4-phthalaldehydec, 1,4-dicyanobenzene, triethanolamine (TEOA) were obtained from Energy Chemical. Dithiooxamide was obtained from Acros Organics. Cesium carbonate (Cs_2CO_3), lithium bis(trimethylsilyl)azanide (1.0 mol/L in THF), terephthalaldehyde were obtained from Aladdin Chemical. Other reagents of analytical gradewere utilized without further purification.

1.2 Characterization

Fourier-transformed infrared (FT-IR) spectra were collected on KBr disks in transmission mode using Affinity-1S FTIR spectrometer. Ultraviolet–visible spectra were measured on a UV-VIS-NIR spectrophotometer (UV-2600, Shimadzu Japan). Photoluminescence (PL) spectra of the catalysts were recorded by F-4600 Fluorescence Spectrophotometer with excitation wavelength at 315 nm. The Time-resolved photoluminescence spectra (TAS) were obtained on an Edinburgh FLS980 Spectrometer with an EPL laser at λex = 375 nm and a xenon arc lamp. ^{13}C cross polarization magic angle spinning nuclear magnetic resonance (^{13}C CP/MAS NMR) spectra were recorded on a WB 400 MHz Bruker Avance II spectrometer with the contact time of 2 ms (ramp 100) and pulse delay of 4 s. Surface area, N_2 adsorption isotherms (77 K) and pore size distributions were measured using Micromeritics ASAP 2020 Plus surface area and porosity analyzer. Before analysis, the samples were degassed at 120 °C for 10 h under vacuum (10^{-5} bar). The surface areas were calculated based on nitrogen adsorption isotherms by Brunauer-Emmett-Teller (BET) or Langmuir analysis. Pore size distributions were calculated by DFT methods via the adsorption branch. Thermogravimetric analysis (TGA) was performed using an SDT Q600 (TA, America). The samples were heated at the rate of 10 °C/min under a nitrogen atmosphere up to 800 °C. The microstructural properties of electrode materials were characterized by X-ray diffraction using the Cu Kα radiation (λ = 1.5418 Å) (XRD, Rigaku Mini Flex 600). Transmission electron microscopy (TEM) images of the material were obtained with JEOL JEM-2100 transmission electron microscope. Polymer morphologies were investigated with a Zeiss SIGMA field emission scanning electron microscope (SEM). Before measurement, the samples were sputter coated with platinum. The samples were dispersed in ethanol and ultrasonicated for 6 h at 25 °C and then two drops of suspension were taken onto the mica sheet and allowed to dry. X-ray photoelectron spectroscopy (XPS) analysis was conducted on an Al Kα X-ray source (1486 eV, Nexsa, Thermal Fisher). High-resolution valence band ultraviolet photoelectron spectra (UPS) were obtained from Thermal Fisher Nexsa.

1.3 Electrochemical measurements

Electrochemical properties of the crystalline CTFs were measured using a three-electrode system in a chemical workstation with a brand of CHI760E, Chenhua. For the measurements, CTF samples (2 g) were firstly dispersed in 1% Nafion ethanol solution (5 ml) and then ultrasonic 20 min. After that, 100 μL suspension was deposited on the FTO plate to act as the working electrode, while Ag/AgCl electrode worked as the reference electrode and Pt flake acted as the counter electrode.

0.2M Na_2SO_4 aqueous solution acted as electrolyte during the measurements. Electrochemical impedance spectroscopy (EIS) frequency ranged from 1 Hz to 105 Hz and the photocurrents were measured under visible light irritation with an interval of 30 second, while the Mott-Schottky curves were recorded at 1000 Hz, 1500 Hz and 2000 Hz, respectively. A 0.2 M Na_2SO_4 solution (pH = 2.5) was used as the electrolyte. A 300 W Xenon lamp with a 420 and 520 nm cut-off filter was used as the light source during the measurement. The applied potentials vs. Ag/AgCl is converted to RHE potentials using the following equation:

$$E_{RHE} = E_{\frac{Ag}{AgCl}} + 0.0591pH + E^{\theta}_{\frac{Ag}{AgCl}} \left(E^{\theta}_{\frac{Ag}{AgCl}} = 0.199\,V \right) \quad \text{(S1)}$$

1.4 Photocatalytic hydrogen production

50 mg of CTF powder was added in 100 ml aqueous solution which contained 10 ml TEOA. It was further ultrasonicated for 30 min to obtain a well-dispersed suspension. Hexachloroplatinic acid (27 µl, 3 wt% aqueous solution) as a co-catalyst was added to the solution. The resulting suspension was transferred into the reactor top-irradiation reaction vessel connected to a closed gas system. The reaction mixture was evacuated several times to ensure complete removal of air prior to irradiation with a 300 W Xe light-source (Perfect light, PLS-SXE300). Time duration of the photocatalytic hydrogen production is 5 h. Hydrogen evolved from the system was detected every hour using Ar_2 as carrier gas through gas chromatography (FULI, GC-2020) equipped with a thermal conductivity detector (TCD) referencing against standard gas with a known concentration of hydrogen. Hydrogen dissolved in the reaction mixture was not measured and the pressure increase generated by the evolved hydrogen was neglected in the calculations. The cycling photocatalytic test is similar to the single photocatalytic run with a duration of 5 hours each cycle. Between each cycle, the reaction system was evacuated for 15 min.

1.5 The calculations of apparent quantum yield

AQE is calculated by the following formula:

$$AQE = \frac{2 \times number\ of\ evolved\ H_2\ molecules}{number\ of\ incident\ photons} \times 100\% = \frac{2 \times CN_A}{Pt\lambda/hc} \times 100\% \quad \text{(S2)}$$

where C is the amount of H_2 evolution per hour; λ is the irradiation light wavelength, N_A is the Avogadro constant; h is the plank constant, c is light speed, t is the light irradiation time, and P is the incident light intensity.

1.6 DFT Calculations

Density functional theory (DFT) calculations were performed using $DMol^3$ code in Materials Studio. The exchange-correlation energy was calculated within the generalized gradient approximation (GGA) using PBE functional. The OBS method for DFT-D correction was employed for the description of the van der Waals dispersion interactions. The valence electron functions were expanded into a set of numerical atomic orbitals by a double numerical basis with polarization functions (DNP). Taking the relativistic effect into account, the density functional semi-core pseudopotential (DSPP) method was employed for S atoms, whereas the carbon, oxygen, and hydrogen atoms were treated with an all-electron basis set. A Fermi smearing of 0.005 Ha and a real

space cutoff of 4.4 Å were used to improve the computational performance.

2. Synthetic Procedures

2.1 Synthesis of terephthalamidine dihydrochloride[1]:

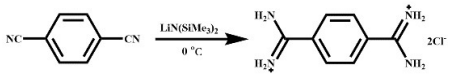

To a solution of 1,4-Dicyanobenzene (1.28 g, 10.0 mmol) in 20 mL THF, 40 mL of 1 M $LiN(SiMe_3)_2$ solution was added dropwise in 30 min at 0 °C. The mixture was stirred at 25 °C for 3 h and then cooled to 0 °C. The reaction was quenched by careful addition of 6 M HCl–EtOH (40 mL) and the mixture was set aside overnight. The precipitate was then filtered, washed with Et_2O, and then the powder was recrystallized from H_2O–EtOH mixture. Yield: (2.24 g, 95%). ^{1}H NMR (400MHz, DMSO-d^6): δ = 9.63 (s, 4H, NH), 9.36 (s, 4H, NH), 8.03 (s, 4H, aromatic H).

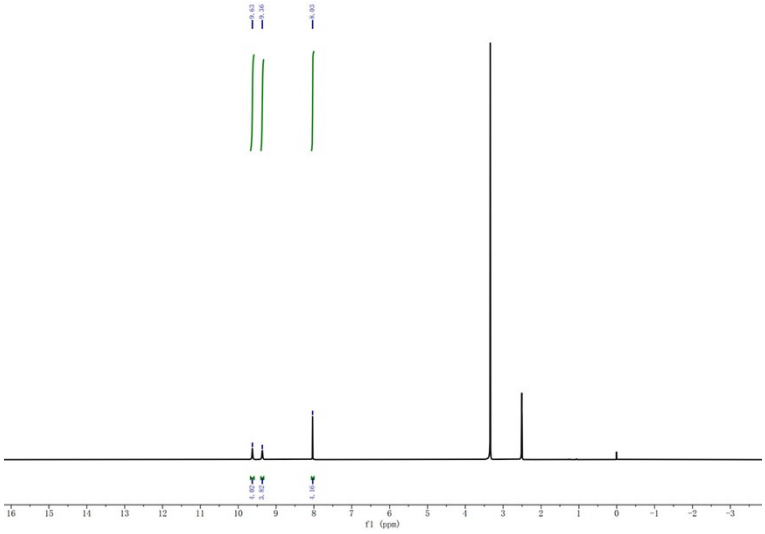

Figure S1. ^{1}H NMR (DMSO-d^6) of terephthalamidine dihydrochloride.

2.2 Synthesis of 4,4'-(thiazolo[5,4-d]thiazole-2,5-diyl)dibenzaldehyde (TzDA)[2]:

To a solution of 1,4-phthalaldehyde (670.0 mg, 5.0 mmol) in DMF (30 mL) was added a solution of dithiooxamide (60.0 mg, 0.5 mmol) in DMF (10 mL) dropwise to result in a mixture which was heated at 150 ℃ for 5 h. The precipitates formed were collected by filtration, and subjected to chromatography (petroleum ether/EtOAc = 3:1) to afford TzDA (82 mg, 47%). ^{1}H NMR (400 MHz, $CDCl_3$): δ=10.12 (s, 2H), 8.22 (d, J = 8.2 Hz, 4H), 8.04 (d, J = 8.3 Hz, 4H).

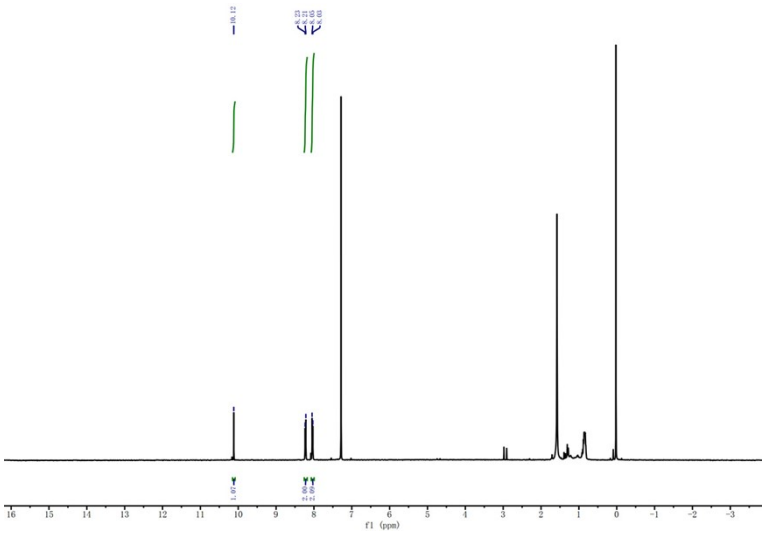

Figure S2. ^{1}H NMR ($CDCl_3$) of TzDA.

2.3 Synthesis of [1,1':4',1''-Terphenyl]-4,4''-dicarbaldehyde[3]:

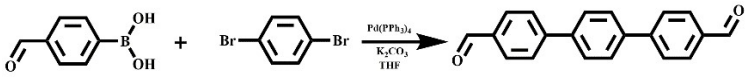

To an oven dried round bottomed flask equipped with stirrer bar was added 1,4-dibromobenzene (2.00 g, 8.48 mmol, 1.0 eq.) and 4-formylphenylboronic acid (3.05 g, 20.35 mmol, 2.4 eq.) before being dissolved in THF (100 mL). This solution was degassed (Ar_2 bubbling, 30 mins) prior to the addition of a 2M aqueous K_2CO_3 solution (50.9 mL, 101.74 mmol, 12.0 eq.) and $Pd(PPh_3)_4$ (392 mg, 0.34 mmol, 0.04 eq.). The reaction was heated at reflux (80 °C) for 18 h before being allowed to cool to room temperature, at which point a large quantity of small crystals formed. These crystals were collected by filtration under reduced pressure. The resulting filtrate was diluted with Et_2O (300 mL), yielding an additional, larger crop of crystals which were again recovered via filtration under reduced pressure and combined with the initial crop to afford the desired target product as beige crystals which were used without further purification (2.10 g, 7.33 mmol, 86%).^{1}H NMR (400 MHz, $CDCl_3$): δ 10.10 (s, 2H), 8.01 (d, J = 8.2 Hz, 4H), 7.84 (d, J = 8.3 Hz, 4H), 7.79 (s, 4H).

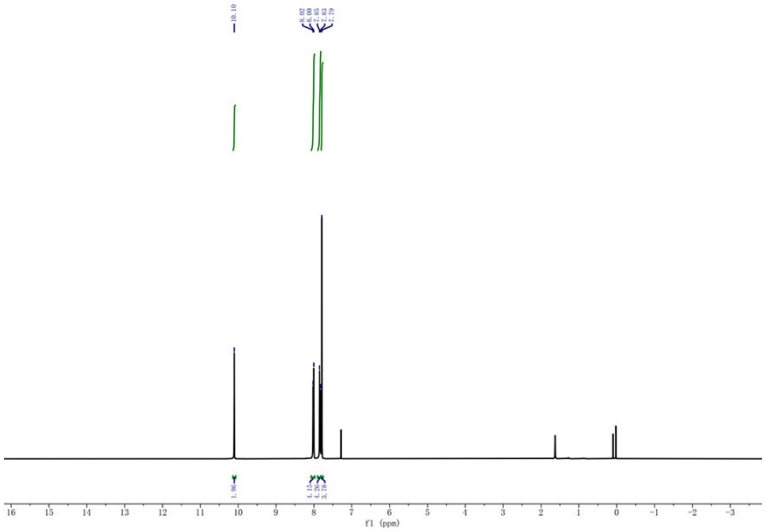

Figure S3. ^{1}H NMR ($CDCl_3$) of [1,1':4',1''-Terphenyl]-4,4''-dicarbaldehyde.

2.4 Synthesis of CTF-NWU-1:

CTF-NWU-1 was synthesized based on modification of protocols reported by Yuan et al.[4] First, 0.50 g NH_2-f-SiO_2 were dissolved in 10 mL solvent (DMSO/o-DCB=1/1, V/V) and ultrasonically dispersed at normal temperature until uniform. Then, 0.023 g TZDA was dissolved in the above solution respectively and stirred at 60 °C for 12 h. After that, 0.03 1 g terephthalamidine dihydrochloride and 0.132 g cesium carbonate were added to the re action system and reacted at 60 and 80 °C for 12 h respectively to obtain the prepolymer with core–shell structure. Finally, 0.074 g TZDA, 0.099 g terephthalamidine dihydrochlorid e and 0.265 g cesium carbonate were added to the above reaction system and reacted at 100 and 120 °C for 24 h respectively. The obtained products was washed twice with deio nized water and DMF for 5 h each time, and the last time was washed with deionized w ater, then collected by centrifugation and finally freeze-dried for 24 h. The product was th en stirred overnight in 1% HF solution, filtered by extraction, and washed with plenty of water until neutral to obtain the final product. And then freeze dried to result in CTF-NW U-1 as a yellow power (145.9 mg, 78% yield).

2.5 Synthesis of CTF-NWU-2:

The synthesis method of CTF-NWU-2 is the same as that of CTF-NWU-1.

3. Supplementary Figures and Tables

Table S1. Synthesis of the CTF-NWU-1 under variable conditions.

Entry	Solvent	Temperature and Time	Base	S_{BET}	Template
1	DMSO (5 ml)	60℃、80℃、100℃ respectively react for 12 hours, 120℃ reaction 3d	Cs_2CO_3 (397.3 mg)	32.12 $m^2 \cdot g^{-1}$	-
2	DMSO (5 ml)	100℃、120℃、140℃ respectively react for 12 hours, 160℃ reaction 3d	Cs_2CO_3 (397.3 mg)	37.67 $m^2 \cdot g^{-1}$	-
3	DMSO:O-DCB (2.5 ml : 2.5 ml)	100℃、120℃、140℃ respectively react for 12 hours, 160℃ reaction 3d	Cs_2CO_3 (397.3 mg)	326.08 $m^2 \cdot g^{-1}$	-
4	DMSO:O-DCB (2.5 ml : 2.5 ml) NaCl (3 g) 未研磨	100℃ react 24h, 140℃ reaction 24h, 160℃ reaction 2d	Cs_2CO_3 (397.3 mg)	44.43 $m^2 \cdot g^{-1}$	-
5	DMSO:O-DCB (2.5 ml : 2.5 ml) NaCl (3 g) 研磨	100℃ react 24h, 140℃ reaction 24h, 160℃ reaction 2d	Cs_2CO_3 (397.3 mg)	172.93 $m^2 \cdot g^{-1}$	-
6	DMSO:Mesitylene (2.5 ml : 2.5 ml)	100℃、120℃、140℃ respectively react for 12 hours, 160℃ reaction 3d	Cs_2CO_3 (397.3 mg)	318.33 $m^2 \cdot g^{-1}$	-
7	DMSO:Toluene (2.5 ml : 2.5 ml)	100℃、120℃、140℃ respectively react for 12 hours, 160℃ reaction 3d	Cs_2CO_3 (397.3 mg)	287.45 $m^2 \cdot g^{-1}$	-
8	DMSO:O-DCB (2.5 ml : 2.5 ml)	100℃、120℃、140℃ respectively react for 12 hours, 160℃ reaction 3d	KOH (68.4 mg)	20.72 $m^2 \cdot g^{-1}$	-

9	DMSO:O-DCB (2.5 ml : 2.5 ml)	100℃、120℃、140℃ respectively react for 12 hours, 160℃ reaction 3d	t-BuOK (136.9 mg)	89.54 $m^2 \cdot g^{-1}$	-
10	DMSO:O-DCB (2.5 ml : 2.5 ml)	100℃、120℃、140℃ respectively react for 12 hours, 160℃ reaction 3d	Triethylamine (0.2 ml)	81.68 $m^2 \cdot g^{-1}$	-
11	DMSO:O-DCB (2.5 ml : 2.5 ml)	100℃、120℃、140℃ respectively react for 12 hours, 160℃ reaction 3d	Cs_2CO_3 (397.3 mg)	488.10 $m^2 \cdot g^{-1}$	0.25 g
12	DMSO:O-DCB (2.5 ml : 2.5 ml)	100℃、120℃、140℃ respectively react for 12 hours, 160℃ reaction 3d	Cs_2CO_3 (397.3 mg)	253.89 $m^2 \cdot g^{-1}$	0.50 g
13	DMSO:O-DCB (2.5 ml : 2.5 ml)	100℃、120℃、140℃ respectively react for 12 hours, 160℃ reaction 3d	Cs_2CO_3 (397.3 mg)	168.32 $m^2 \cdot g^{-1}$	0.75 g
14	DMSO:O-DCB (2.5 ml : 2.5 ml)	100℃、120℃、140℃ respectively react for 12 hours, 160℃ reaction 3d	Cs_2CO_3 (397.3 mg)	103.68 $m^2 \cdot g^{-1}$	1.00 g

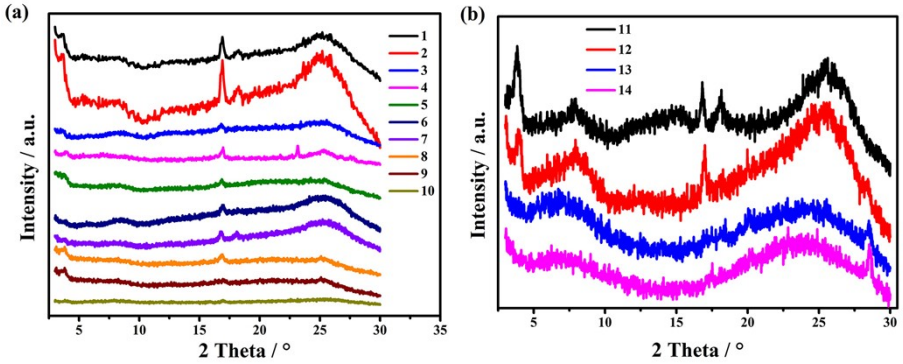

Figure S4. PXRD patterns of CTF-NWU-1 under different conditions.

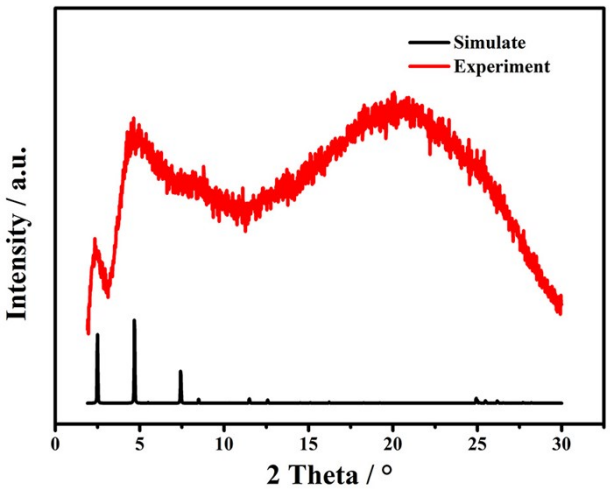

Figure S5. Experimental and simulated PXRD patterns of CTF-NWU-2.

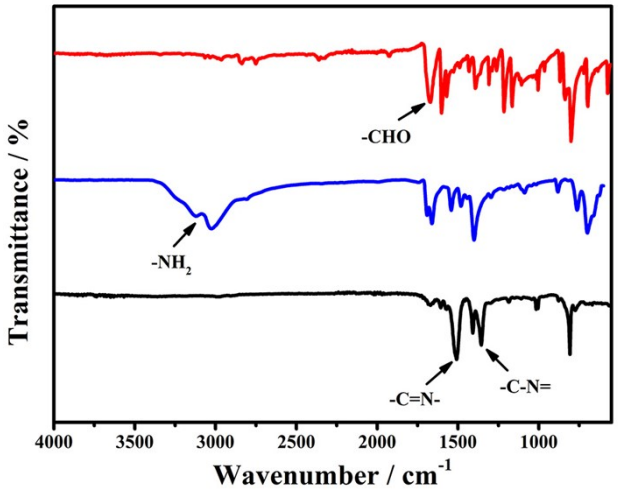

Figure S6. FT-IR spectra of CTF-NWU-2. (Black for CTF-NWU-2, blue for terephthalamidine dihydrochloride, red for1,4-di(4-formylphenyl)benzene)

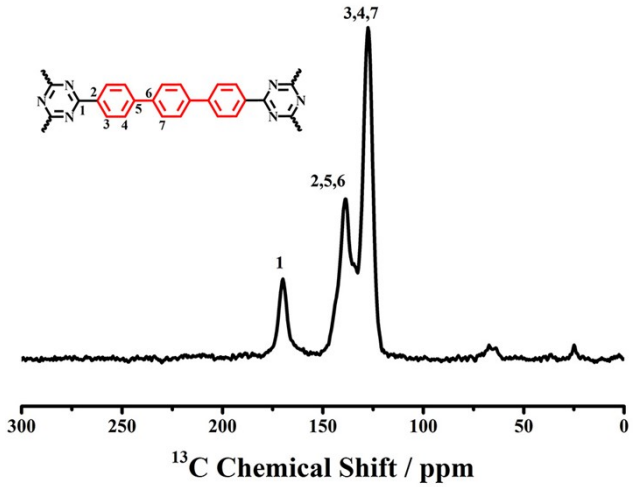

Figure S7. Solid-state ^{13}C CP-MAS NMR of CTF-NWU-2.

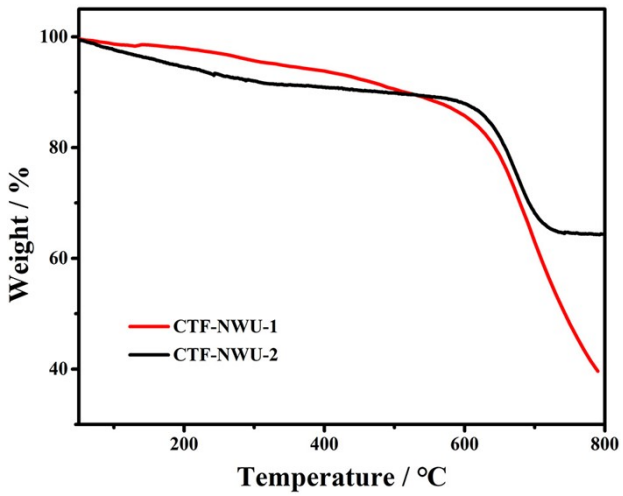

Figure S8. TGA profile of CTF-NWU-1 and CTF-NWU-2 under N_2 atmosphere.

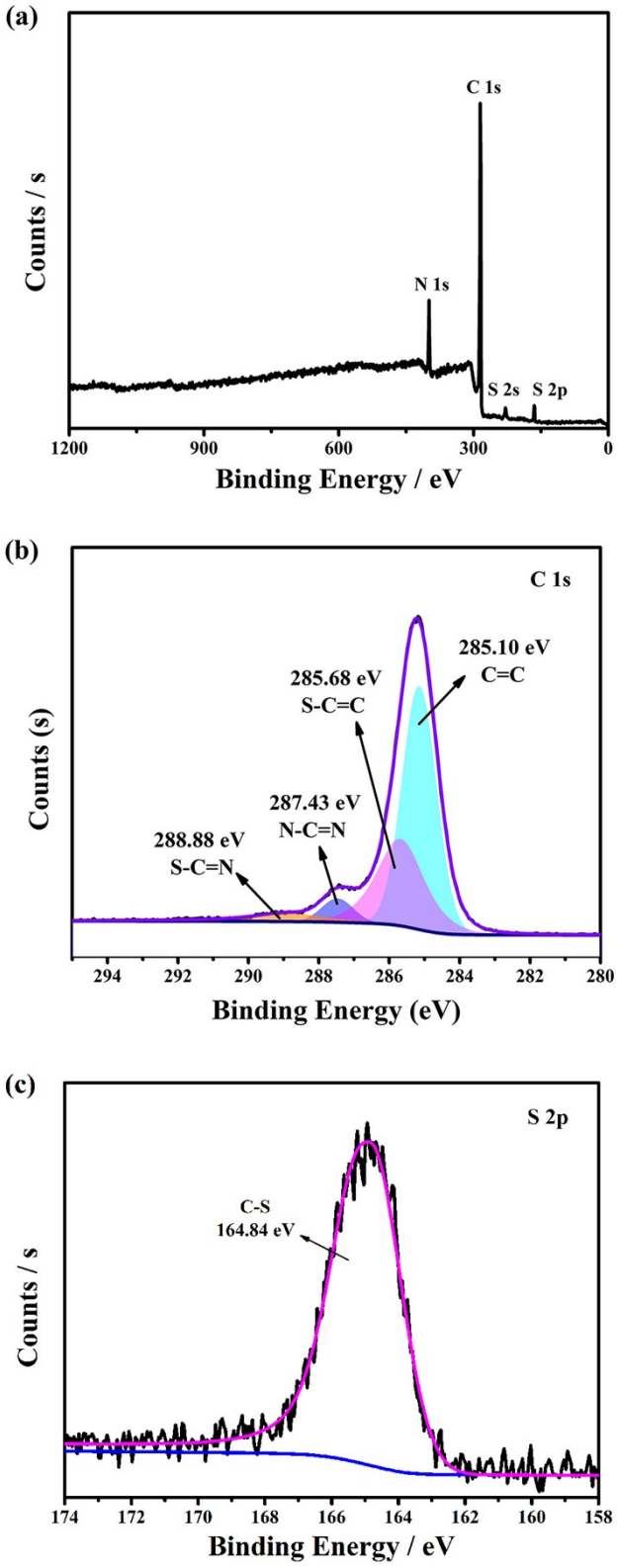

Figure S9. (a) XPS survey spectrum and high-resolution XPS spectra of the **(b)** C 1 s and **(c)** S 2p of CTF-NWU-1.

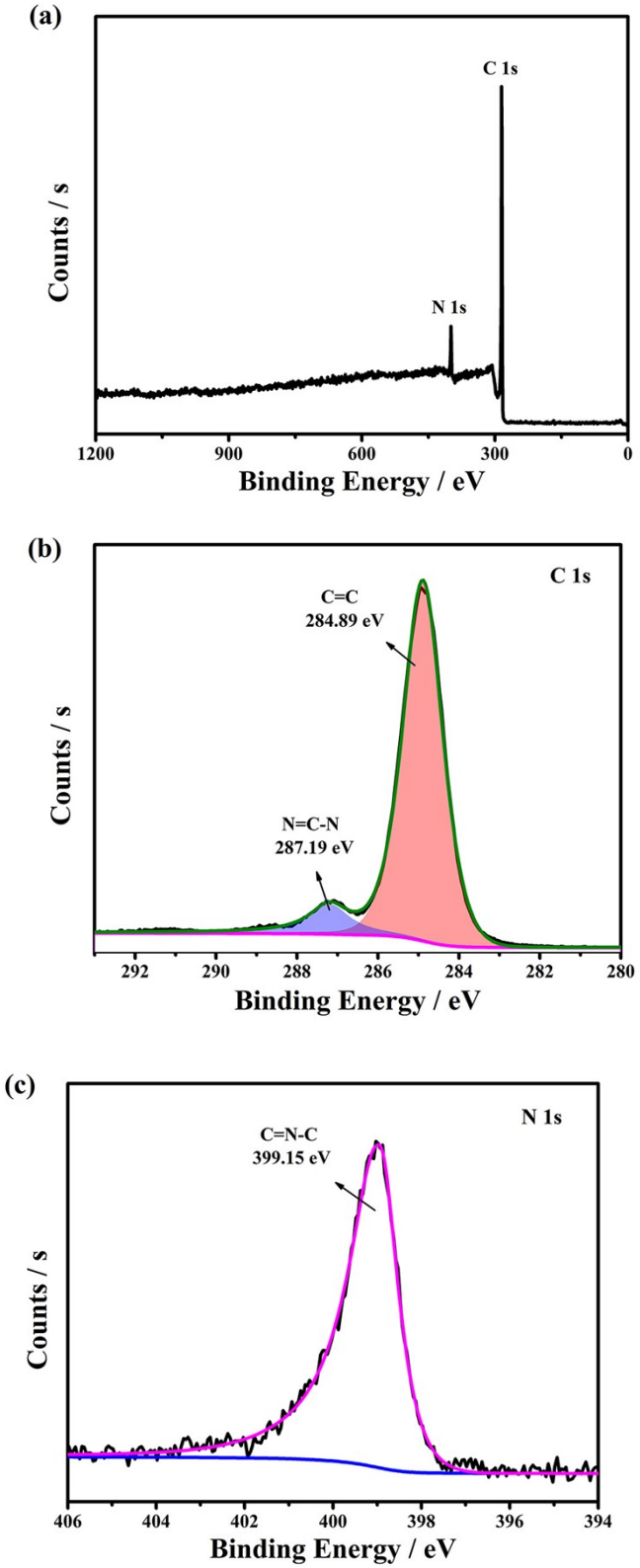

Figure S10. (a) XPS survey spectrum and high-resolution XPS spectra of the **(b)** C 1 s, and **(c)** N 1 s of CTF-NWU-2.

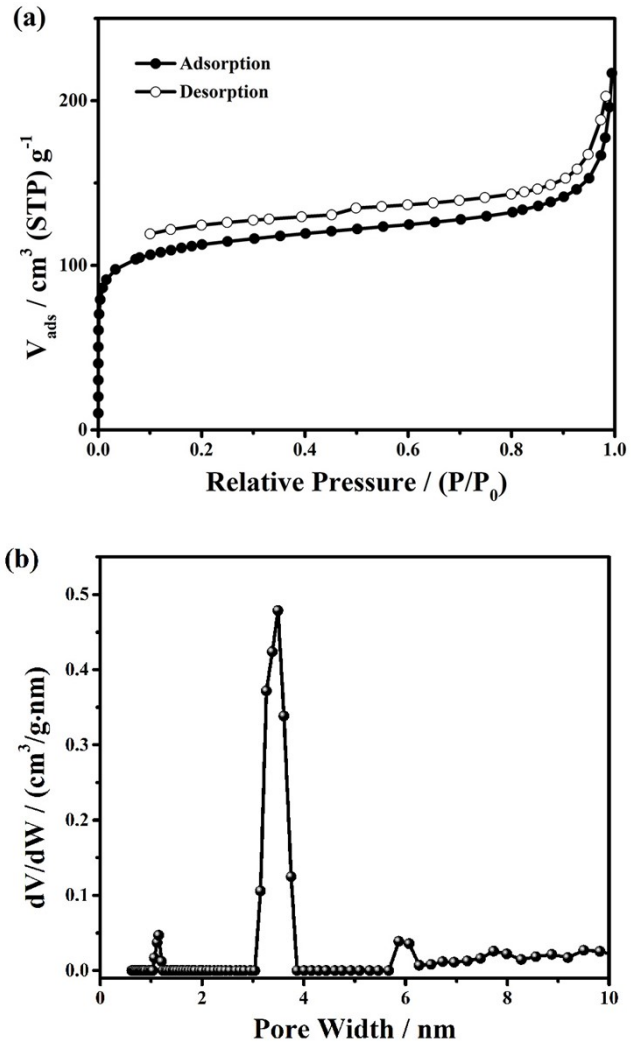

Figure S11. (a) N_2 sorption isotherms and **(b)** pore size distribution curves of CTF-NWU-2.

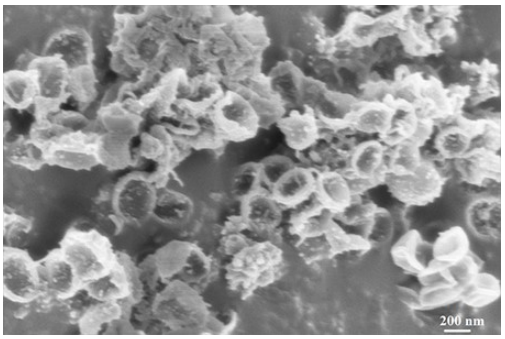

Figure S12. SEM image of CTF-NWU-2.

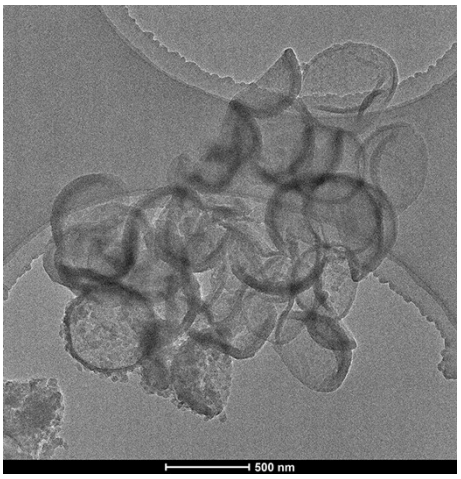
500 nm

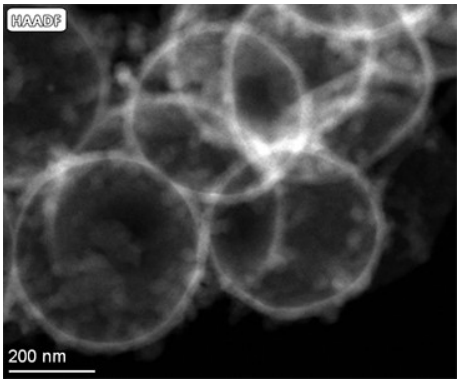
HAADF
200 nm

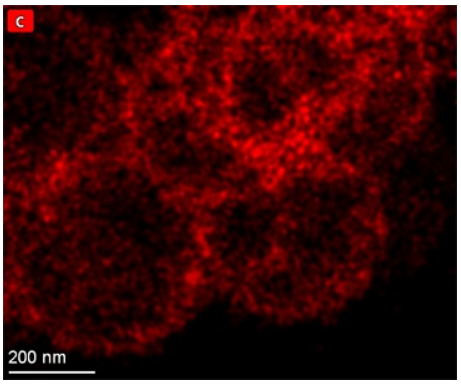
C
200 nm

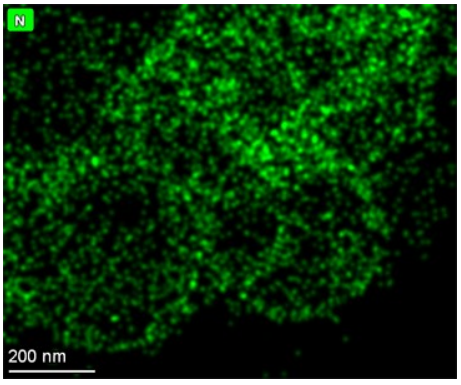
N
200 nm

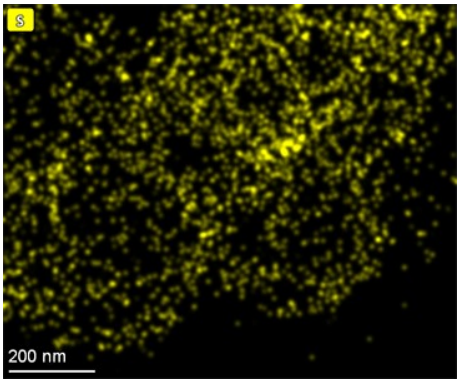

Figure S13. TEM image and elemental mappings of CTF-NWU-1.

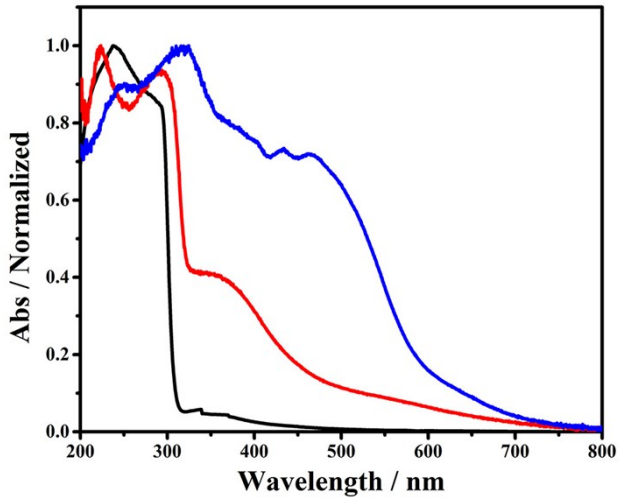

Figure S14. UV-Vis diffuse reflectance absorption spectra (DRS) of TzDA (blue) terephthalamidine dihydrochloride (red), [1,1':4',1"-Terphenyl]-4,4"-dicarbaldehyde (black).

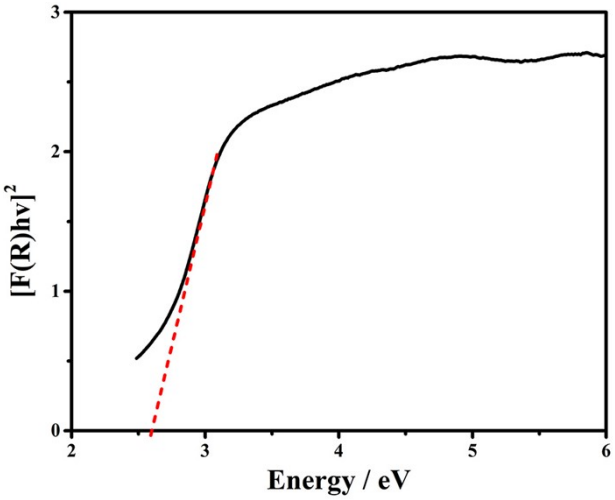

Figure S15. Band gaps of CTF-NWU-2 determined by the Kubelka-Munk-transformed reflectance spectra.

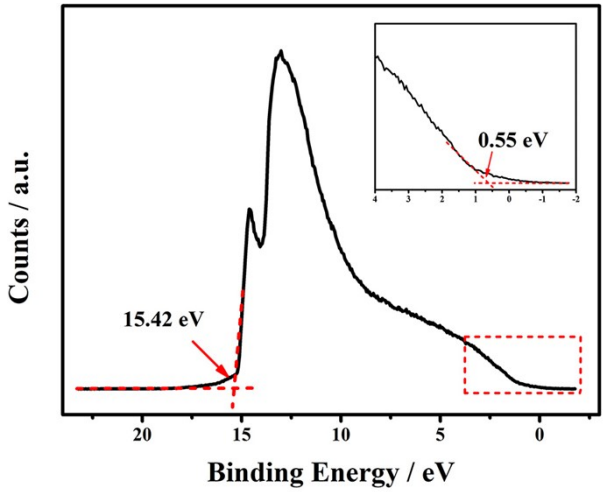

Figure S16. UPS spectra of CTF-NWU-2.

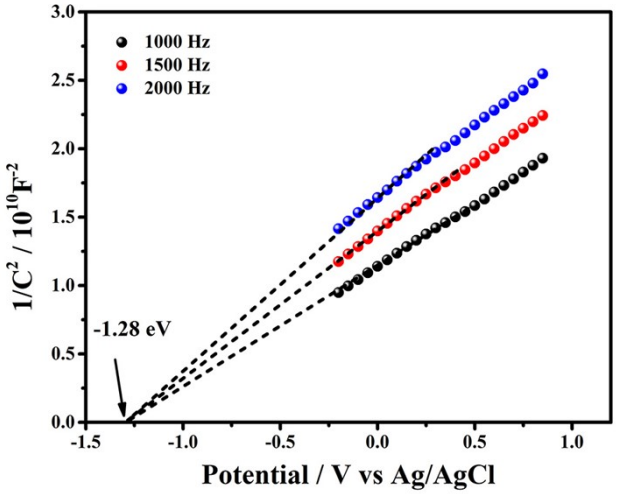

Figure S17. Mott-Schottky plots of CTF-NWU-2.

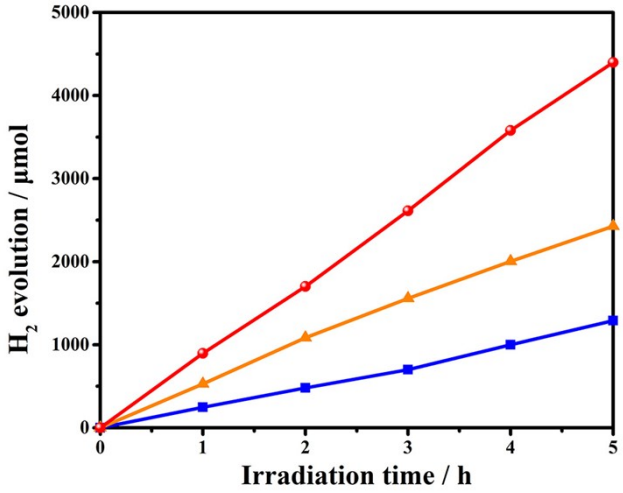

Figure S18. Photocatalytic hydrogen production of CTF-NWU-1 under different platinum cocatalyst deposition methods. (The red line is the sodium borohydride reduction deposition

method, the orange line is the photoreduction deposition method, and the blue line is the direct deposition method.)

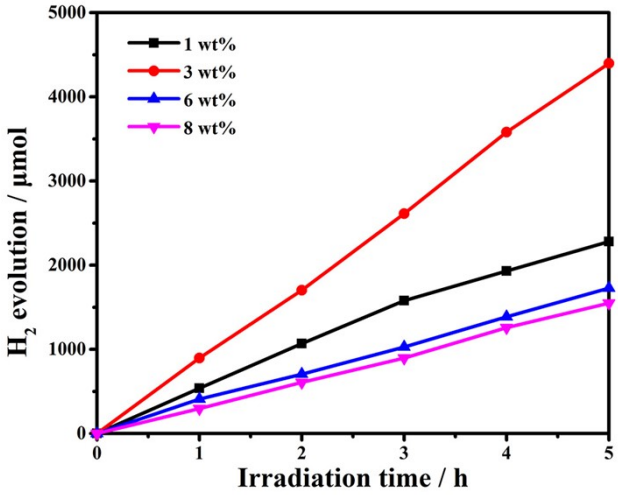

Figure S19. Hydrogen precipitation reaction of CTF-NWU-1 with different loadings of platinum cocatalyst.

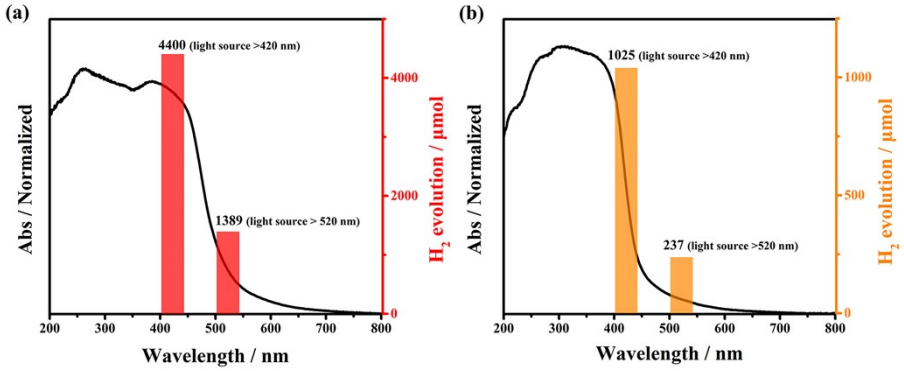

Figure S20. Wavelength-dependent H_2 evolution of photocatalytic hydrogen production by CTF-NWU-1 (a) and CTF-NWU-2 (b).

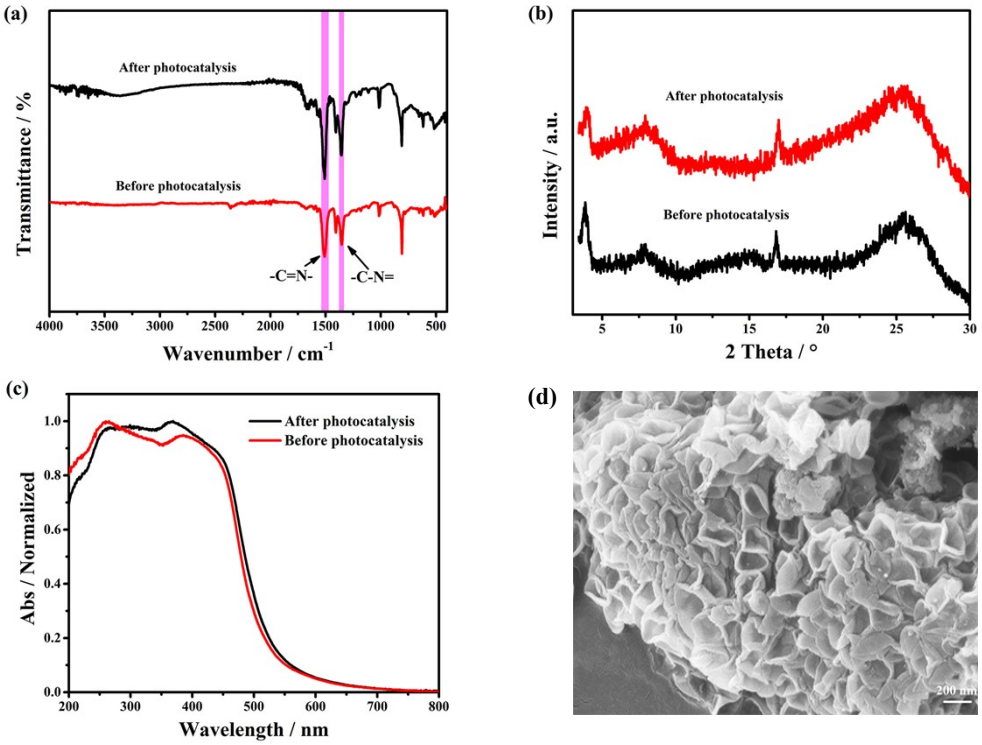

Figure S21. (a) FT-IR spectra, (b) PXRD patterns, (c) UV-Vis diffuse reflectance absorption spectra (DRS), (d) SEM image of CTF-NWU-1 after photocatalytic cycle hydrogen production.

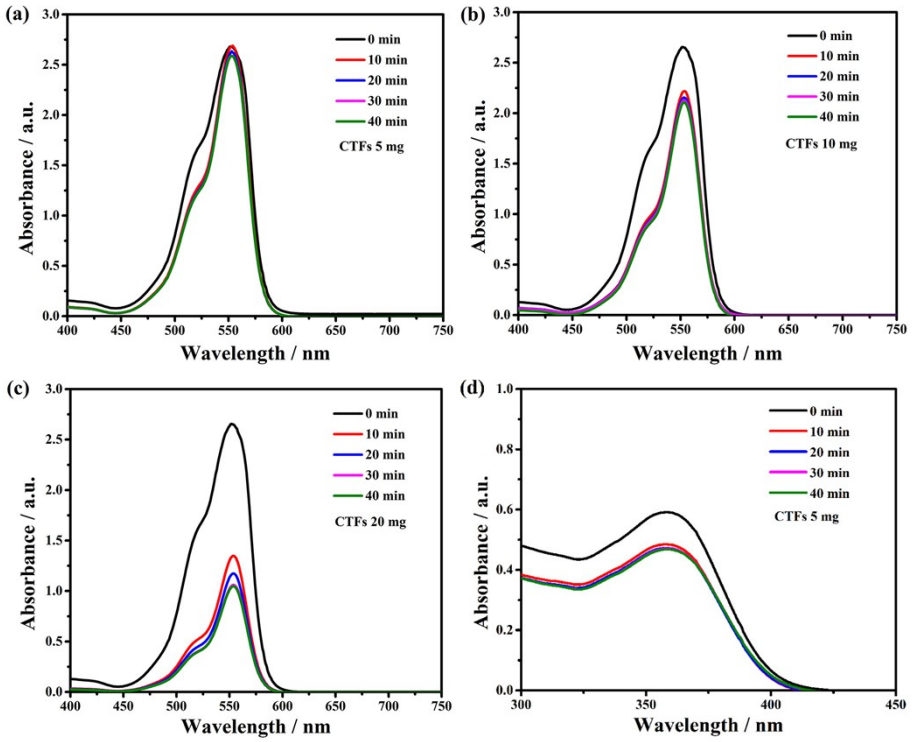

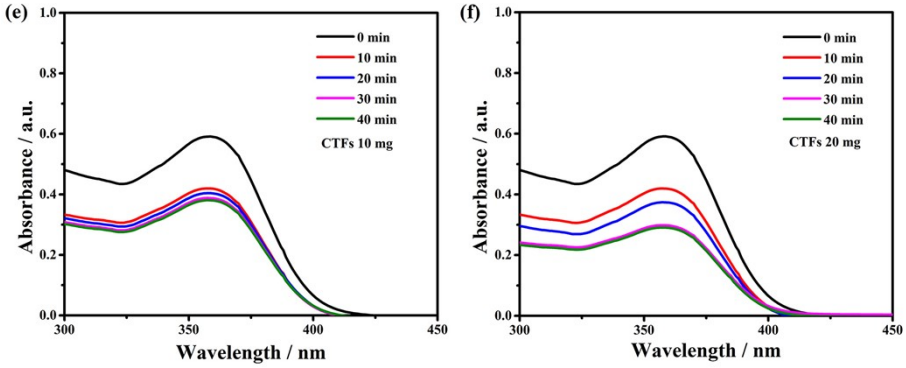

Figure S22. Verify the time required for CTF-NWU-1 adsorption and desorption to reach equilibrium under dark adsorption, (a-c) is rhodamine B, (d-f) is tetracycline hydrochloride.

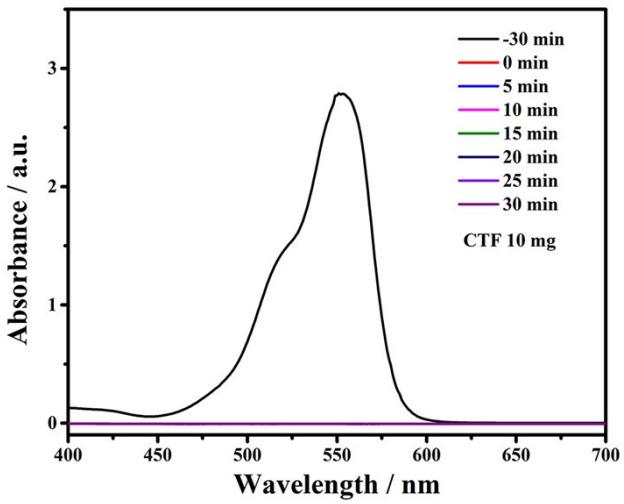

Figure S23. UV−vis spectra of RhB (20 mg·L^{-1}) after different illumination time intervals in the presence of CTF-NWU-2 (10 mg).

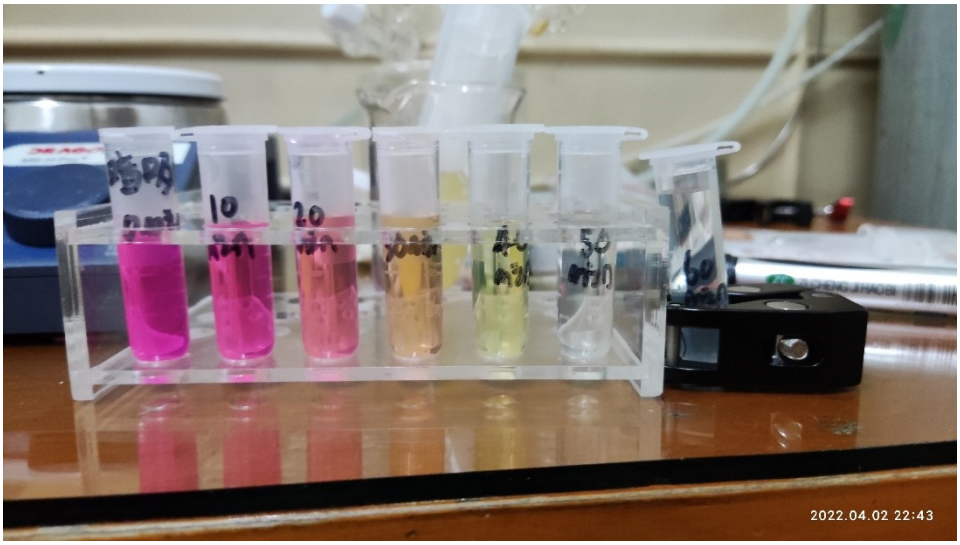

Figure S24. The color change of RhB when CTF-NWU-1 (5 mg) used as catalysts (the interval is 10 min)

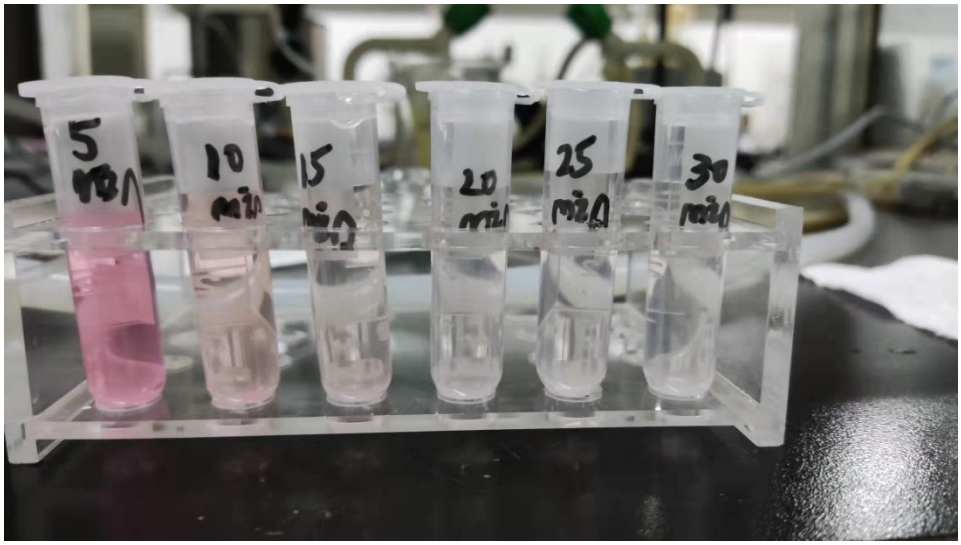

Figure S25. The color change of RhB when CTF-NWU-1 (10 mg) used as catalysts (the interval is 5 min)

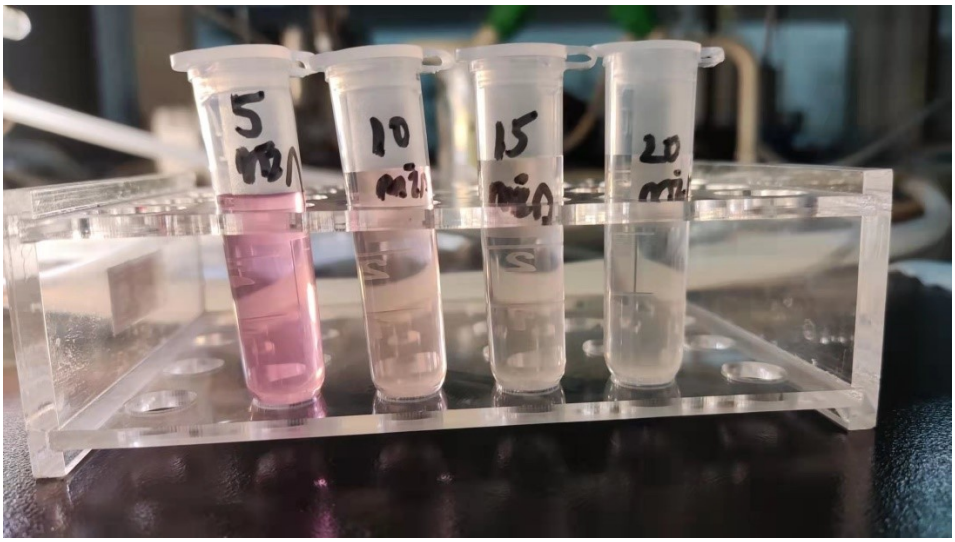

Figure S26. The color change of RhB when CTF-NWU-1 (20 mg) used as catalysts (the interval is 5 min)

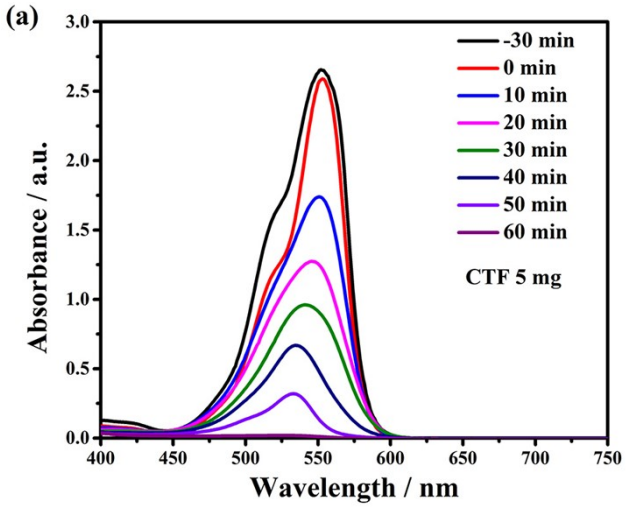

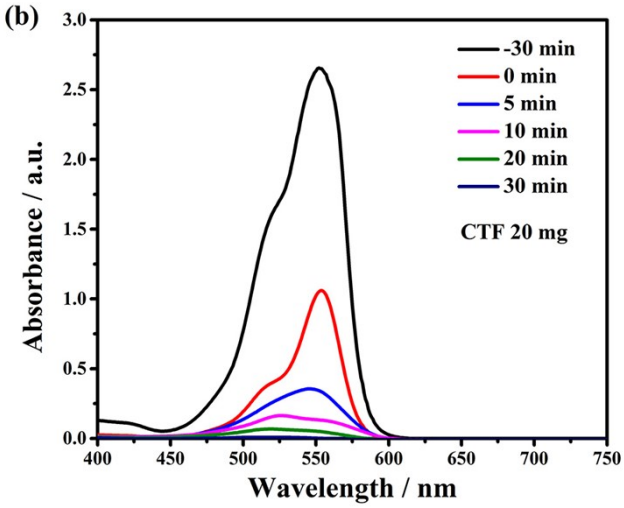

Figure S27. UV−vis spectra of RhB (20 mg·L^{-1}) after different illumination time intervals in the presence of various CTF-NWU-1 (5 mg and 20 mg).

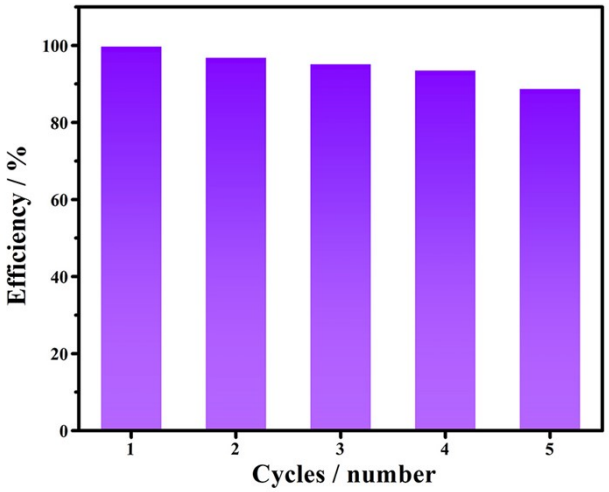

Figure S28. Recyclability test of CTF-NWU-1 for 10 mg catalyst, 10 mg·L^{-1} RhB degradation.

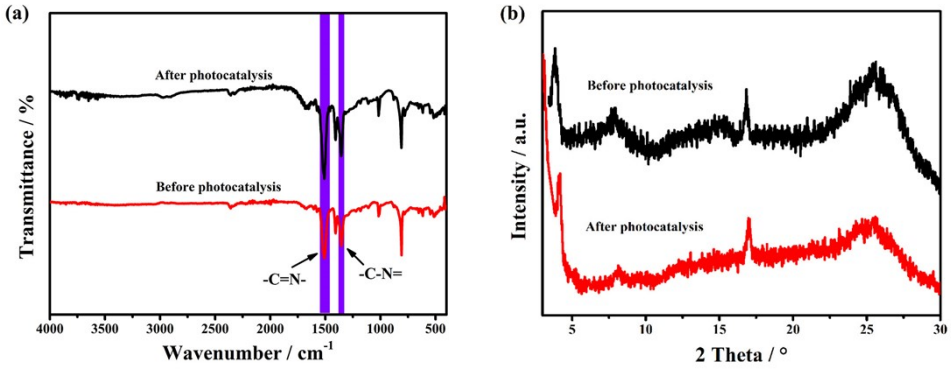

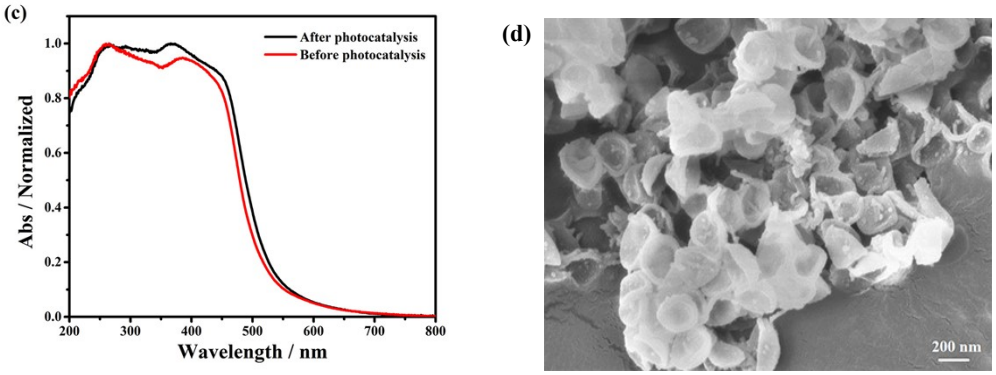

Figure S29. (a) FT-IR spectra, (b) PXRD patterns, (c) UV-Vis diffuse reflectance absorption spectra (DRS), (d) SEM image of CTF-NWU-1 after photocatalytic cycle degradation of rhodamine B.

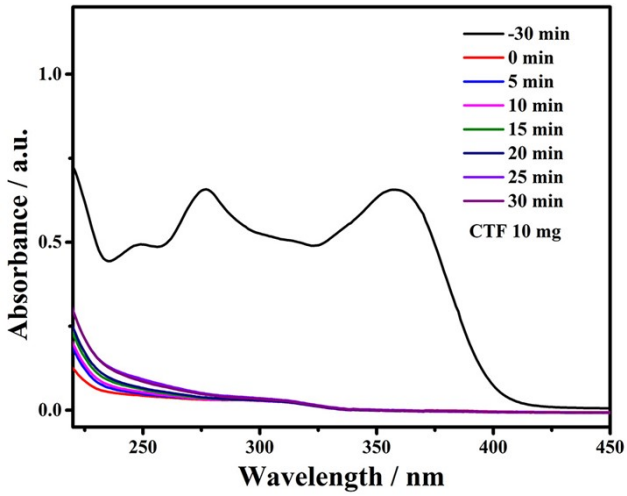

Figure S30. UV−vis spectra of TC (20 mg·L^{-1}) after different illumination time intervals in the presence of CTF-NWU-2 (10 mg).

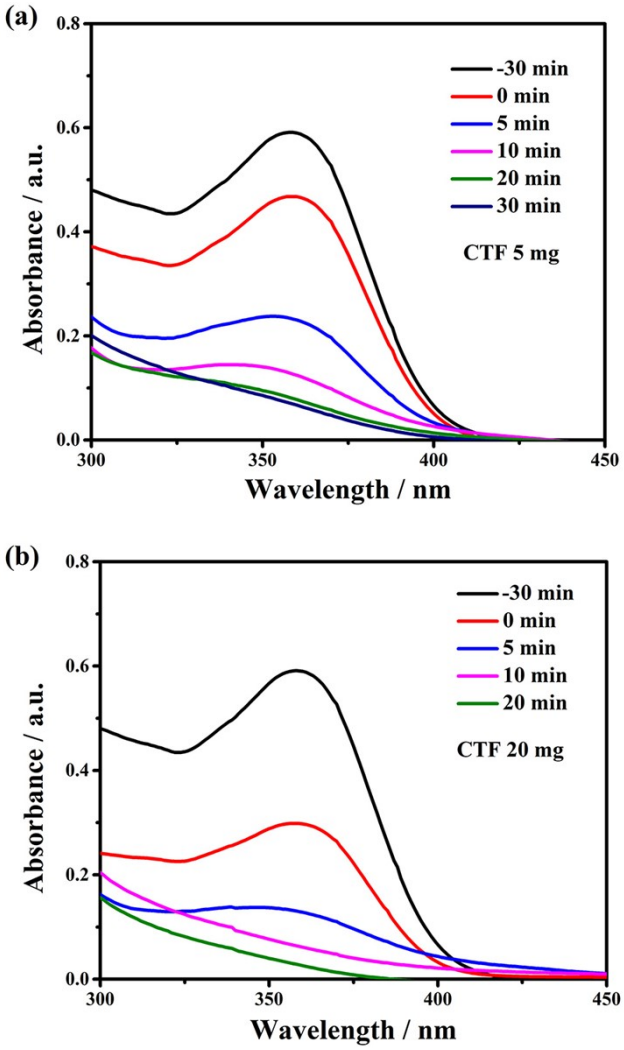

Figure S31. UV−vis spectra of TC (20 mg·L^{-1}) after different illumination time intervals in the presence of various CTF-NWU-1 (5 mg and 20 mg).

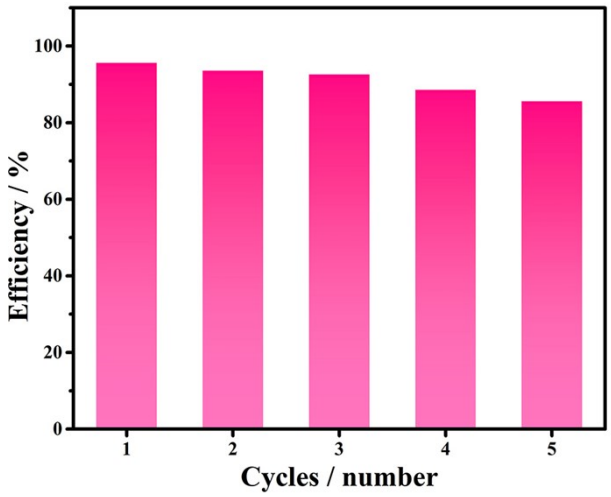

Figure S32. Recyclability test of CTF-NWU-1 for 10 mg catalyst, 20 mg·ml^{-1} TC degradation.

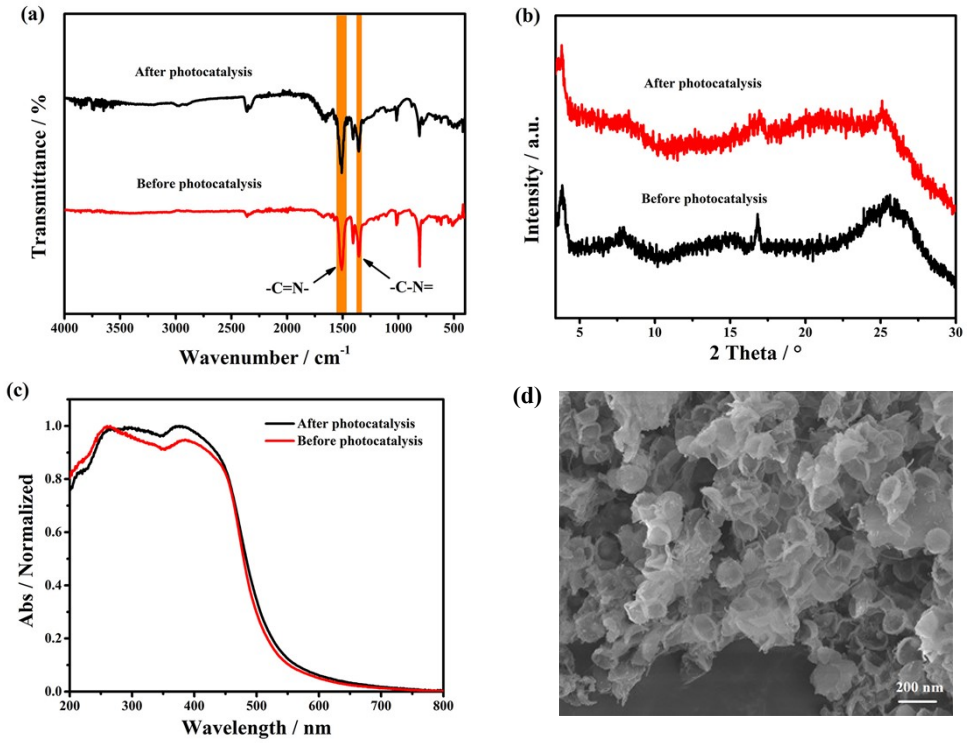

Figure S33. (a) FT-IR spectra, (b) PXRD patterns, (c) UV-Vis diffuse reflectance absorption spectra (DRS), (d) SEM image of CTF-NWU-1 after photocatalytic cycle degradation of TC.

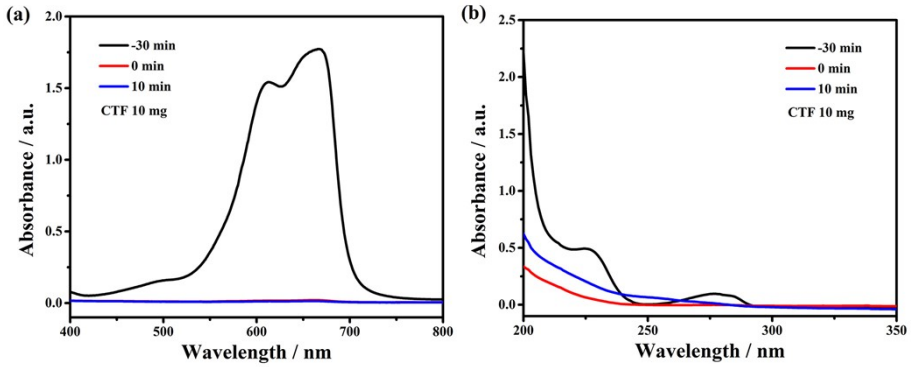

Figure S34. UV−vis spectra of (a) MB (20 mg·L^{-1}) and (b) BPA (20 mg·L^{-1}) after different illumination time intervals in the presence of CTF-NWU-1 (10 mg).

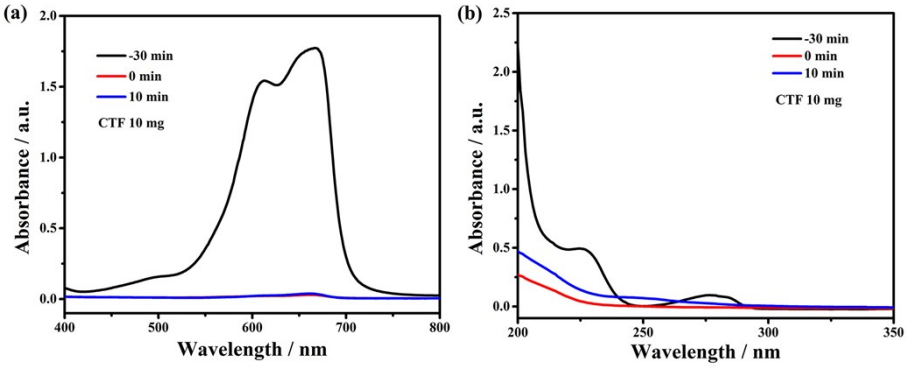

Figure S35. UV−vis spectra of (a) MB (20 mg·L^{-1}) and (b) BPA (20 mg·L^{-1}) after different illumination time intervals in the presence of CTF-NWU-2 (10 mg).

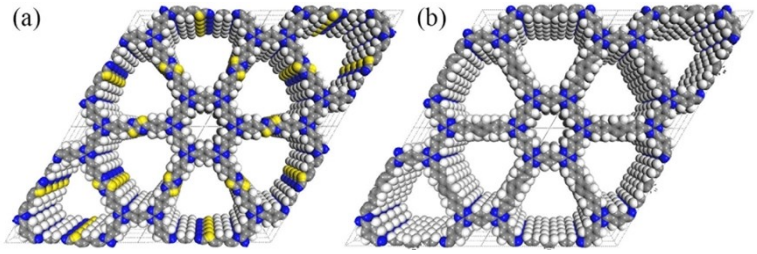

Figure S36. (a) and (b) are the 3D perspective views of CTF-NWU-1 and CTF-NWU-2, respectively.

Table S2. Summarized representative metal-free activated photocatalysts for H_2 production

Photocatalyst	The loadings of Pt element	H_2 evolution rate ($\mu mol \cdot h^{-1} \cdot g^{-1}$)	Reference
g-C_3N_4	-	3	[5]
Pt-PVP-TP-COF	6 wt%	8420	[6]
N3-COF	3 wt%	1703	[7]
FS-COF	8 wt%	10100	[8]
CTF1-10min	-	1083	[9]
g-$C_{40}N_3$-COF	-	580	[10]
S-CTF	1 wt%	2000	[11]
P-CTF	1 wt%	500	[12]
Cl-CTF	3 wt%	1300	[13]
CTF-Cl	1 wt%	1500	[14]
CTFs	3 wt%	2600	[15]
CTF-HUST-S3	3 wt%	791	[16]
CTF-BT/Th-1	3 wt%	6600	[17]
PETZ-COF	3 wt%	7324	[18]
CTF-NWU-1	3 wt%	17600	This Work

Table S3. Elemental analysis of terephthalamidine dihydrochloride.

EA(wt%)	Exp.	Cal.
C	37.7	40.9
H	4.7	5.1
N	20.4	23.8
Cl	27.5	30.2

Table S4. Elemental analysis of TzDA.

EA(wt%)	Exp.	Cal.
C	57.2	61.7
H	3.3	2.9
N	8.5	8.0
S	16.8	18.3

Table S5. Elemental analysis of [1,1':4',1''-Terphenyl]-4,4''-dicarbaldehyde.

EA(wt%)	Exp.	Cal.
C	79.7	83.9
H	4.5	4.9
O	12.3	11.2

4. Supplementary References

1 Y. Shu, H. Lei, Y.-N. Tan, M. Meng, X.-C. Zhang and C. Liu, *Dalton Trans.*, 2014, **43**, 14756–14765.

2 W.-Q. Li, X.-F. Huang, T.-W. Zeng, Y.-A. Liu, W.-B. Hu, H. Yang, Y.-B. Zhang and K. Wen, *Angew. Chem., Int. Ed.*, 2021, **60**, 1869−1874.

3 R. L. Greenaway, V. Santolini, M. J. Bennison, B. M. Alston, C. J. Pugh, M. A. Little, M. Miklitz, E. G. B. R. Eden-Rump, A. Clowes, H. J. Shakil, H. Cuthbertson, M. E. Armstrong, K. E. Briggs and A. Cooper, *Nat. Commun.*, 2018, **9**, 2849-2860.

4 Y.-C. Yuan, B. Sun, A.-M. Cao, D. Wang and L.-J. Wan, *Chem. Commun.*, 2018, **54**, 5976-5979.

5 X. Wang, K. Maeda, A. Thomas, K. Takanabe, G. Xin, J.-M. Carlsson, K. Domen and M. Antonietti, *Nat. Mater.*, 2009, 8, 76-80.

6 J.-T. Ming, A. Liu, J.-W. Zhao, P. Zhang, H.-W. Huang, H. Lin, Z.-T. Xu, X.-M. Zhang, X.-X. Wang, J. Hofkens, M.-J. Roeffaers and J.-L. Long, *Angew. Chem.*, 2019, **131**, 18458–18462.

7 V. S. Vyas, F. Haase, L. Stegbauer, G. Savasci, F. Podjaski, C. Ochsenfeld and B. Lotsch, *Nat. Commun.*, 2015, **6**, 8508.

8 X. Wang, L. Chen, S.-Y. Chong, M. A. Little, Y.-Z. Wu, W.-H. Zhu, R. Clowes, Y. Yan, M.-A. Zwijnenburg, R.-S. Sprick and A. Cooper, *Nature. Chem.*, 2018, **10**, 1180–1189.

9 S. Kuecken, A. Acharjya, L. Zhi, M. Schwarze and R. S. Thomas, *Chem. Commun.*, 2017, **53**,

10 S. Bi, C. Yang, W. Zhang, J. Xu, L. Liu, D. Wu, X. Wang, Y. Han, Q. Liang and F. Zhang, *Nat. Commun.*, 2019, **10**, 2467.

11 L. Li, W. Fang, P. Zhang, J. Bi, Y. He, J. Wang and W. Su, *J. Mater. Chem. A*, 2016, **4**, 12402-12406.

12 Z. Cheng, W. Fang, T. Zhao, S. Fang, J. Bi, S. Liang, L. Li, Y. Yu and L. Wu, *ACS Appl. Mater. Interfaces.*, 2018, **10**, 41415-41421.

13 S. Li, M. Wu, T. Guo, L. Zheng, D. Wang, Y. Mu, Q. Xing and J. Zou, *Appl. Catal. B: Environ.*, 2020, **272**, 118989.

14 Z. Cheng, K. Zheng, G. Lin, S. Fang, L. Li, J. Bi, J. Shen and L. Wu, *Nanoscale Adv.*, 2019, **1**, 2674–2680.

15 K. Wang, L. Yang, X. Wang, L. Guo, G. Cheng, C. Zhang, S. Jin, B. Tan and A. Cooper, *Angew. Chem., Int. Ed.*, 2017, **56**, 14149-14153.

16 L. Guo, X. Wang, Z. Zhan, Y. Zhao, L. Chen, T. Lu, B. Tan and S. Jin, *Chem. Mater.*, 2021, **33**, 1994–2003.

17 W. Huang, Q. He, Y.-P. Hu and Y.-G. Li, *Angew. Chem., Int. Ed.*, 2019, **131**, 8768-8772.

18 H.-P. Yu, J.-Z. Zhang, X.-R. Yan, C.-G. Wu, X.-R. Zhu, B.-W. Li, T.-F. Li, Q.-Q. Guo, J.-F. Gao, M.-J. Hu and J. Yang, *J. Mater. Chem. A*, 2022, advance article.